FEASIBILITY STUDY INTO THE IDENTIFICATION OF LANDMINES USING UWB RADAR: AN ANALYSIS USING SYNTHESIZED DATA

J. LoVetri[1,2], S. Primak[1], B.J.A.M. van Leersum[2], and A.P.M. Zwamborn[2]

[1]Department of Electrical Engineering
The University of Western Ontario,
London, Ontario, Canada N6A 5B9

[2]TNO Physics and Electronics Laboratory
P.O. Box 96864, 2509 JG Den Haag, The Netherlands

INTRODUCTION

The goal of this research is to detect and identify buried land mines (LM). The technique being investigated is the use of ultra-wideband (100 MHz to 3 GHz) ground penetrating radar (UWB/GPR). The first step is to gain an understanding of the scattered signal received from the use of such a system. A major point of interest is: which electromagnetic scattering features and signal processing techniques can be used in the detection/identification process? Possible candidates of scattering features are late-time resonances and diffusion poles, whereas signal processing techniques are synthetic aperture radar (SAR) imaging [1], correlation and/or E-pulse receivers [2]. It is important to have good detection and identification algorithms, which work well in the ideal situation, before one can deal with the practical situation, in which there will be uncertainty in various physical parameters such as: the local electrical characteristics of the ground, the local heterogeneity of the ground (rocks, layers, tree and plant roots), surface roughness of the ground and covering foliage, position (depth and orientation) of the LM, and relative position of the radar with respect to the ground and the LM. Thus, in this work, we investigate the post-processing of impulse type radar signals, where the signals are synthesized, for relatively ideal situations, using the finite-difference time-domain (FDTD) technique. Much has been published about this technique so the details will be left for the references [3].

Both the ground and the LM's are modelled as lossy dielectrics. Synthetic impulse responses are obtained using a multistatic configuration (*i.e.* one transmitter point above the ground, many receiver points just above the ground). First we construct SAR images from the multistatic impulse responses. The effect of the air-ground interface is partially removed by running the FDTD code without the LM (system response), as well as with the LM (target response), and then deconvolving the system response from the target response. This produces an approximation for the impulse response for the LM itself.

Ultra-Wideband, Short-Pulse Electromagnetics 4
Edited by Heyman *et al.*, Kluwer Academic / Plenum Publishers, New York, 1999.

As a possible identification technique, the complex natural resonances of the radar responses are tabulated for various angles. Prony's method is used to extract the late-time poles from the radar signals.

FDTD SIMULATIONS OF THE GPR PROBLEM

The geometry of the problem which was analyzed using the FDTD technique is shown in Figure 1. A cubical mesh of size 100X100X100 having a cell size of 1 cm was used. A transient dipole (**S1** or **S2** in the figure), modelled by an ideal y-directed current source which is 1 cm in length, is located above a lossy ground at grid location (50, 40, 50) for **S1** and location (65, 40, 50) for **S2**, as shown. Only one source was used during any run of the FDTD code. A lossless dielectric cube is placed in the ground and the electric field is sampled at test points **T1-T9** which are 1 cm above the ground. The electrical parameters of the cube and the ground are as shown in Figure 1.

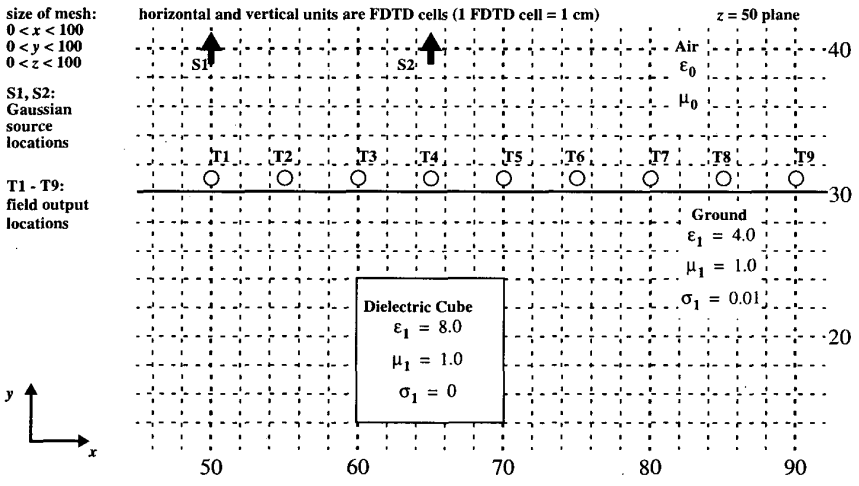

Figure 1. FDTD geometry for buried dielectric cube inside a lossy ground. The horizontal and vertical units are FDTD cells

The time domain variation of the small dipole, **S1** or **S2**, is given by the derivative of a Gaussian function, specifically:

$$g(t) = \begin{cases} 0, & t < 0 \\ -2((t-t_0)/b^2)\exp(-(t-t_0)^2/b^2), & t \geq 0 \end{cases} \tag{1}$$

with $b = 5 \times 10^{-10}$ s, and $t_0 = 2 \times 10^{-9}$ s. A scaled version of this waveform and its Fourier transform are shown in Figure 2. Example plots of the electric fields calculated at some of the observation points are shown in Figure 3.

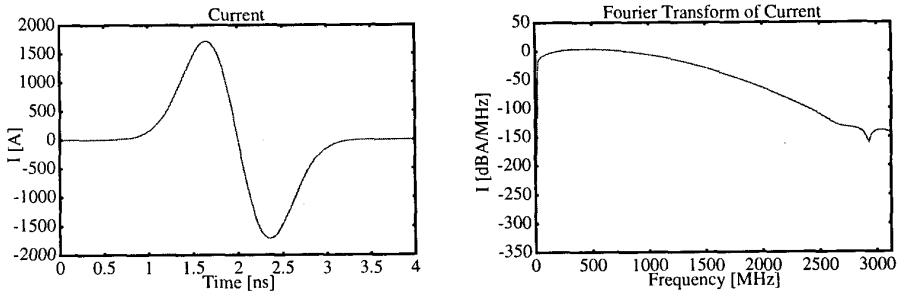

Figure 2. Current waveform and its Fourier transform.

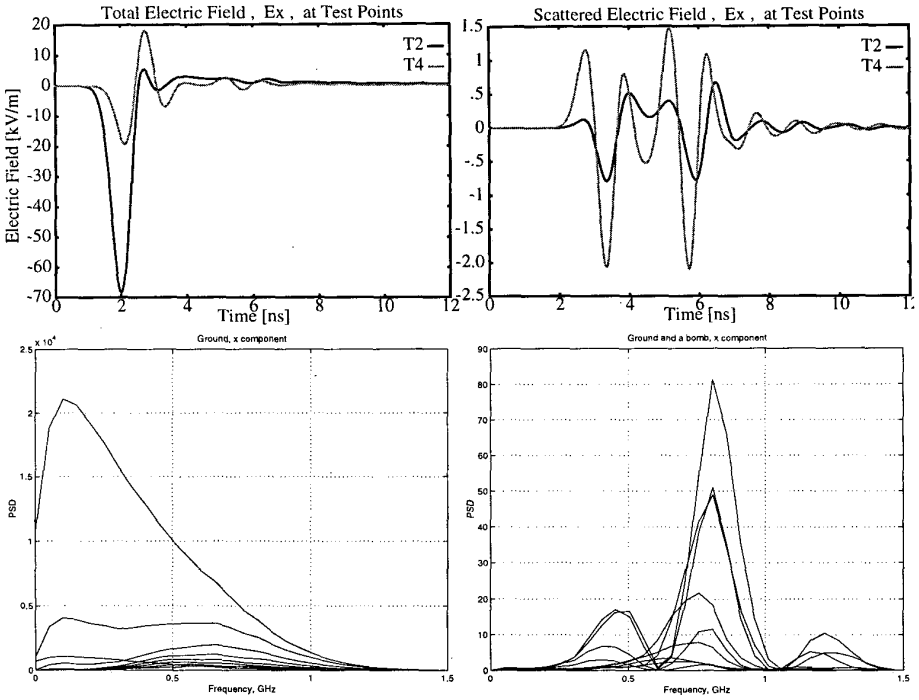

Figure 3. Top: example fields at the observation points: T2 and T4. Bottom: Fourier transform of E_x fields at all observation points. Left: Total fields; Right: Scattered Fields.

ISAR IMAGING

As the first step we have built a set of classical bistatic ISAR imaging [4], assuming that time-domain signal, received at each observation point corresponds to a specific angle of arrival of reflected waves. The following reconstruction algorithms can be found in [4]

$$f_m(\rho, \theta) = \int_{\phi_{min}}^{\phi_{max}} R_m[\rho\cos(\theta - \phi)]d\phi \qquad (2)$$

for monostatic measurements, and

$$f_b(\rho, \theta) = \int_{\beta_{min}}^{\beta_{max}} R_b\left[\rho \cos\left(\theta - \frac{\phi}{2}\right)\right] d\phi \tag{3}$$

for bistatic measurements. Here $R_m(t)$ is the monostatic target range profile in the time-domain, taken at aspect angle ϕ, ρ and θ are polar coordinates in the image plane. Observations (slices) are available for aspect angles between ϕ_{min} and ϕ_{max}. $R_b(t)$ is the bistatic target range profile which is measured in the bistatic angular range of β_{min} to β_{max}. As can be seen from equations (2) and (3) the procedure for image reconstruction using bistatic measurements is exactly the same as for monostatic imaging except that instead of rotating the image by the angle of observation and then backprojecting, one uses one half of this angle. For the case considered herein, the values of these bistatic angles are unknown since the phase centre of the effective scatterer is unknown. A set of bistatic SAR images were constructed, each assuming a different phase centre of the effective scatterer. The geometry which was used to calculate the bistatic angle is shown in Figure 4. Some of the results are shown in Figure 5.

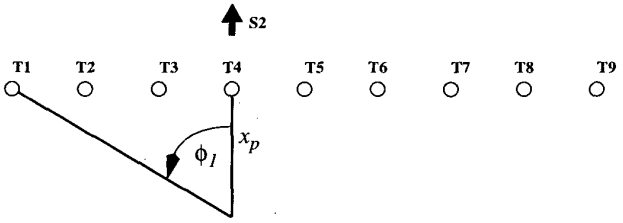

Figure 4. Geometry used to estimate bistatic angles, ϕ_1 to ϕ_9, when source was at **S2**. The distance to the assumed phase centre, x_p, was varied.

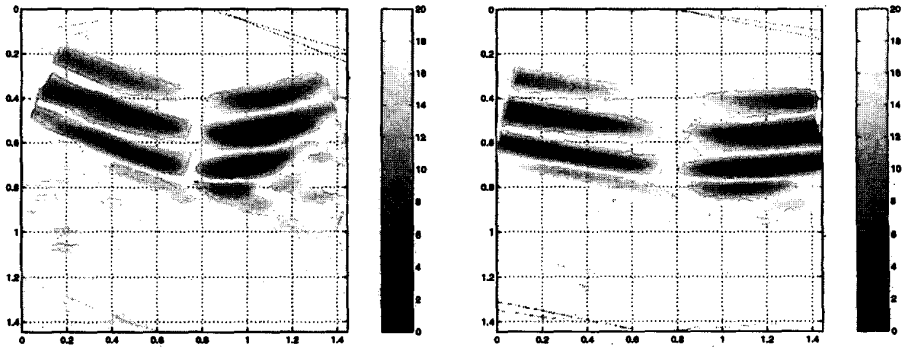

Figure 5. ISAR image corresponding to x_p = 0.75 m, left, and x_p = 1.75 m, right.

PRE-PROCESSING: NEAR-FIELD FOCUSING OF RADAR SIGNALS

The results obtained in the previous section can hardly be considered as satisfactory. This is not surprising since the assumptions inherent in ISAR reconstruction using equations (2-3) are far from being satisfied. First of all, at a single observation point all directions contribute to the scattered field. In this section, an attempt is made to preprocess the

scattering data obtained from the FDTD code to get better compliance with the requirements inherent in the ISAR imaging algorithm summarized by equations (2-3).

The observation points in the previously described problem can be considered as the elements of an antenna array as shown in the Figure 6. Time domain responses $r_k(t)$, $k = 1, \ldots, 9$, measured at each observation point are converted into the frequency domain, and are denoted $R_k(\omega)$. A set of weighting coefficients $w_k^{\phi}(\omega)$ for near-field focusing is developed for every frequency ω and direction of the main lobe ϕ. A combined frequency domain response is calculated as

$$R^{\phi}(\omega) = \sum_{k=1}^{9} w_k^{\phi}(\omega) R_k(\omega) \tag{4}$$

and then converted back to a time domain response using the inverse Fourier transform. A schematic view of the complete procedure is depicted in Figure 7.

The weights, or coefficients $w_k^{\phi}(\omega)$, are developed in such way, that the corresponding directivity of the corresponding antenna array has a maximum at aspect angle ϕ as shown in Figure 6. This can be achieved (see [5]) by setting the magnitude of each coefficient equal to unity

$$\left| w_k^{\phi}(\omega) \right| = 1 \tag{5}$$

and setting the phase using a quadratic dependence on the position n of the element in the array, that is

$$\angle w_k^{\phi}(\omega) = -2\pi f_X' nd + \frac{k}{2r'}(nd)^2 . \tag{6}$$

Here, d is the distance between two sequential elements of the array, $k = \omega/v$ is the wave vector, v is velocity of propagation, f_X' is a spatial frequency related to the aspect angle ϕ and frequency ω as

$$f_X' = \frac{\omega \cos\phi}{2\pi v} . \tag{7}$$

Since this is a near-field design, a distance r' must be specified which gives the distance from the centre of the array at which the focusing is desired. Various values of r' were used, from 10 cm to 1000 m, in order to see the effect in the SAR images.

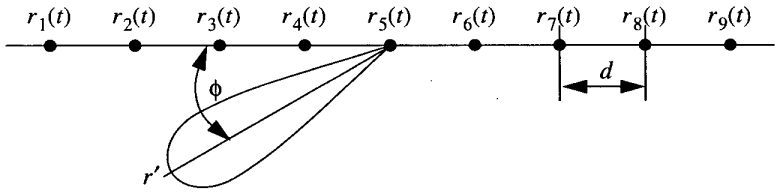

Figure 6. Test points as an antenna array which can be focused to a point in the near-field.

The returned signal, observed at each point, has frequency content limited by the frequency spectrum of the excitation. This reduces the number of frequency bands where the weighting coefficients must be calculated. A typical synthesized time-domain waveform for $\phi = 90°$ is shown in Figure 8. Signals were synthesized for 25 angles, $\phi = 30° \ldots 150°$ in steps of 5° and the corresponding SAR images using these signals are shown in Figure 9 for $r' = 10$ cm, and $r' = 10$ m.

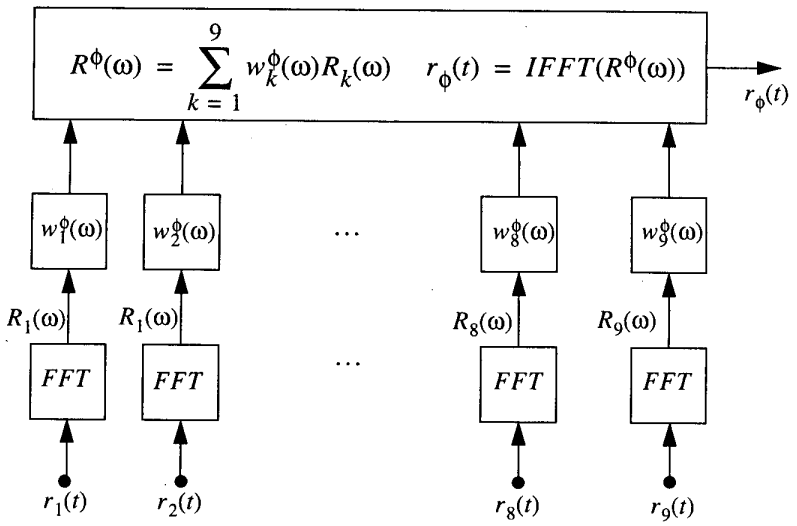

Figure 7. Weighted sum preprocessing of the data.

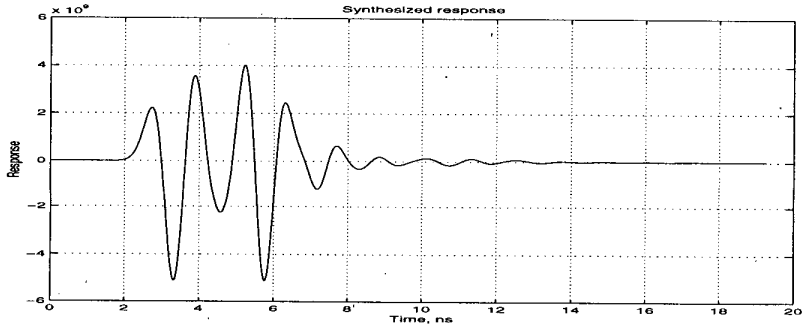

Figure 8. Synthesized signal using near-field focusing algorithm, $\phi = 90°$.

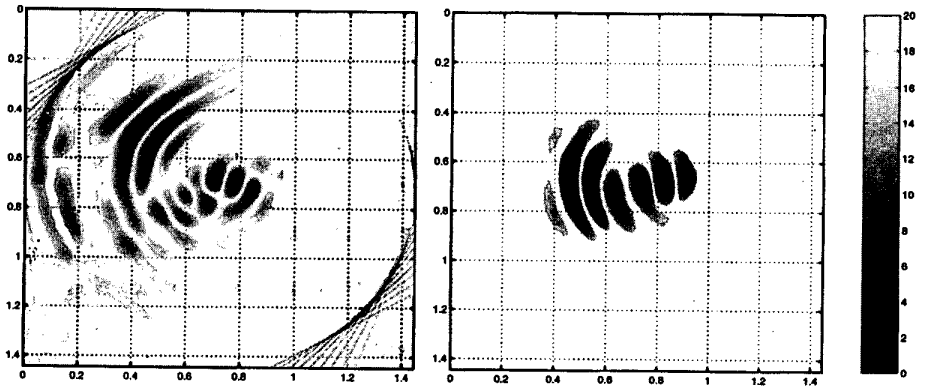

Figure 9. ISAR image obtained using beam-forming algorithm. Left $r' = 10$ cm, Right $r' = 10$ m.

IDENTIFICATION USING LATE-TIME POLES

In frequency ranges where the scatterer produces a considerable natural response (that is, when the wavelength of the incident field is in the order of the size of the target) the late-time scattering response can be approximated as a finite sum of damped sinusoids. The damping time constant and the frequency correspond to complex poles which may be used to identify the scatterer. This is the basis of the so called singularity expansion method (SEM) [6]. According to this model, in the late-time, the time-domain scattered waveform can be represented as

$$r(t) = \sum_{k=1}^{N} A_k \exp(\sigma_k t)\cos(2\pi f_k t + \varphi_k), \; t > T_L. \tag{8}$$

Here, $s_k = \sigma_k + j2\pi f_k$ represent characteristic poles of the target, A_k is the intensity of the corresponding pole, and T_L describes the beginning of late-time at which this model is appropriate. A well known technique for determining the complex poles and residues is Prony's method. The method used is this paper follows that of van Blaricum *et al.* [7, 8].

Before we apply Prony's method to the FDTD data, an attempt is made at removing the system response from the data. The system response is defined as that due to the ground and the source, including the time-domain waveform of the source excitation. A picture of this is shown in Fig. 10. The measured target response can be related to the measured system response and the impulse responses by convolution, that is $s(t)*h(t) = c(t)$. Therefore, in order to obtain the impulse response, $h(t)$, of the target we must deconvolve the system response, $s(t)$, from the measured target response, $\delta(t)$. The procedure we follow for getting the impulse response is the same as that given by Rothwell *et al.* [9].

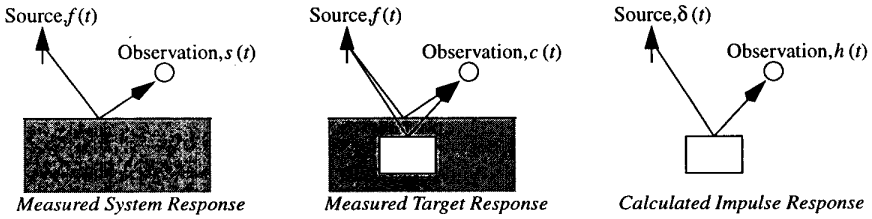

Figure 10. Definition of measured system, measured target, and calculated impulse responses.

Once the impulse response is computed, Prony's method is used to obtain the poles and residues of the late-time portion. The start of the late-time, T_L, is determined in an iterative fashion by varying T_L, computing the damped sinusoid approximation for that T_L using Prony's method, and determining the relative Euclidean norm of the error between the real impulse response and the approximation. When the relative Euclidean norm falls below a specified criterion, we accept the value of T_L as suitable. Example plots of the synthesized system response, the synthesized target response, the calculated impulse response with the approximate signal reconstructed using Prony's method, and the complex poles which were obtained are shown in Figure 11.

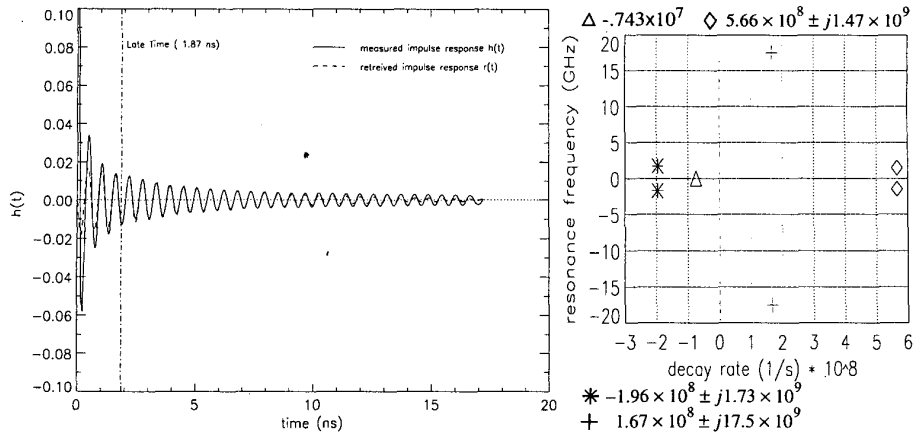

Figure 11. Example plots of the calculated impulse response with the approximate signal reconstructed using Prony's method, and the complex poles for the impulse response.

CONCLUSIONS

Synthetic data of the GPR problem was created using the FDTD technique. Signals for the scattering from various configurations of buried dielectric objects were calculated and SAR images were created from a bistatic set-up consisting of a single wide-band dipole positioned 10 cm above the ground and 9 receiver points just above the ground. A pre-processing algorithm which focuses the scattered signal which was obtained at all 9 observation points was used with the focusing angle and focusing depth chosen at various values to create a set of new signals. The new signals were used to create SAR images of the buried target. This procedure seems feasible for the detection problem since only one wide-band shot was needed, with 9 receiver points. The impulse response at a single receiver point was calculated using a stable deconvolution scheme and Prony's method was applied in order to extract the complex poles. Preliminary investigations are positive that this technique will prove valuable in the identification problem.

REFERENCES

1. E.M. Johansson, J.E. Mast, "Three-dimensional ground penetrating radar imaging using synthetic aperture time-domain focusing," *SPIE* Vol. 2275, pp. 205-214, 1994.
2. L.C. Chan, L. Peters, Jr., D.L. Moffat, "Improved performance of a subsurface radar target identification system through antenna design," *IEEE Trans. AP*, vol. 29, no. 2, pp. 307-311, March 1981.
3. K.S. Kunz and R.J. Luebbers, *The Finite Difference Time Domain Method for Electromagnetics*, CRC Press, 1993.
4. H.-J. Li, and F.-L. Lin, "A generalized interpolation and prediction in microwave imaging involving frequency and angular diversity", *Journal of Electromagnetic Waves and Applications*, Vol. 4, No. 5, 1990, pp. 415-430.
5. L. Ziomek, *Fundamentals of Acoustic Field Theory and Space-Time Signal Processing*, CRC Press, Ann Arbor, 1995.
6. C. Baum, E. Rothwell, K.-M. Chen, and D. Nyquist, "The singularity expansion method and its applications to target identification", *Proc. IEEE*, Vol. 79, No. 10, October, 1991.
7. M.L. van Blaricum, and R. Mittra, " A technique for extracting the poles and residues of a system directly from its transient response," *IEEE Trans. AP*, vol. 23, no. 6, pp. 777-781, 1975.
8. M.L. van Blaricum, and R. Mittra, " Problems and solutions associated with Prony's method for processing transient data," *IEEE Trans. AP*, vol. 26, no. 1, pp. 174-182, 1978.
9. E.J. Rothwell, and W. Sun, "Time domain deconvolution of transient radar data," *IEEE Trans. AP*, vol. 38, no. 4, pp. 470-475, 1990.